ELSEVIER

Surface Science 338 (1995) 94–110

surface science

Laser modifications of Si(100) : Cl surfaces induced by surface melting: etching and cleaning

B. Bourguignon [a,*], M. Stoica [a,1], B. Dragnea [a,1], S. Carrez [a], J. Boulmer [b], J.-P. Budin [b], D. Débarre [b], A. Aliouchouche [b]

[a] *Laboratoire de Photophysique Moléculaire du CNRS, Institut de Physico-Chimie Moléculaire d'Orsay, Bâtiment 213, Université de Paris-Sud, F-91405 Orsay-Cedex, France*

[b] *Institut d'Electronique Fondamentale (associé au CNRS), Bâtiment 220, Université de Paris-Sud, F-91405 Orsay-Cedex, France*

Received 9 November 1994; accepted for publication 29 March 1995

Abstract

Pulsed laser driven modifications of one Cl monolayer (ML) chemisorbed on Si(100) are studied by time of flight mass spectrometry (TOF) of the desorbed molecules, Auger electron spectroscopy (AES) of the modified surface, and Cl depth profile analysis by secondary ion mass spectrometry (SIMS). The experimental conditions are that of surface melting. Evidence of Cl diffusion to the bulk during surface melting, and of strong segregation of Cl in Si during surface recrystallization, are presented. The following branching ratios for 1 Cl ML initially adsorbed on clean Si are measured independently: (a) (from TOF and depth profiler measurements) 0.58 ± 0.07 ML desorb reactively in the form of SiCl and $SiCl_2$. The SiCl to $SiCl_2$ ratio is 1.3 ± 0.3; (b) (from AES measurements) 0.37 ± 0.13 ML are found after the laser pulse in a thin surface layer of 7 atomic planes; (c) (from SIMS measurements) 0.10 ± 0.10 ML are found in deeper layers, the solubility of Cl in solid Si being lower than 10^{19} cm^{-3}, the sensitivity of our SIMS for Cl; (d) 0.12 ± 0.07 ML desorb unreactively in the form of Cl and Cl_2. By order of increasing importance, unreactive desorption, stoichiometry and diffusion to the bulk during the laser pulse have the practical effect of limiting the maximum etch rate to 0.40 ± 0.03 Si ML per laser pulse under the conditions of surface melting. Although the laser pulse induces diffusion of Cl towards the bulk during melting, the strong segregation of Cl during recrystallization limits Si contamination by Cl at undetectable levels to our SIMS. Cl in Si is a very good case for laser cleaning, as is shown by comparison with C and O.

Keywords: Auger electron spectroscopy; Chlorine; Halogens; Laser annealing; Laser etching; Laser surface cleaning; Low index single crystal surfaces; Photon stimulated desorption; Resonance enhanced multiphoton ionization mass spectroscopy (REMPI/MS); Secondary ion mass spectroscopy; Silicon; Surface melting; Surface segregation

1. Introduction

The interaction of a laser beam with a surface on which atoms or molecules are adsorbed may lead to desorption as well as to diffusion to the bulk. Desorption allows for surface etching or cleaning, depending on whether the desorbed molecules contain

* Corresponding author. Fax: +33 1 60 19 25 93; E-mail: bourgnon@psisun.u-psud.fr.

[1] Permanent address: Laser Department, Institute of Atomic Physics, P.O. Box MG-6, Bucharest-Magurele, Romania.

SSDI 0039-6028(95)00518-8

substrate atoms or not. Diffusion leads to ultra-shallow doping, oxidation, compound formation, or bulk contamination, depending on the nature of the incorporated atoms [1,2]. However, the problem of the competition between desorption and diffusion has received little attention despite its important practical consequences (contamination, loss of dopants, etc.); loss of atoms by desorption has been mentioned by some authors, but it has been measured only recently [3] for Ge, B, As and Sb in Si during laser etching experiments; incorporation of O and C in Si was observed in laser cleaning experiments [4]. In this work, we are concerned with diffusion of adsorbates (Cl) during chemical laser etching of Si [5–22]. In this introduction, we first review important results on laser driven diffusion of impurities; next we summarize the literature on Cl adsorption on Si(100) and on laser etching of Si by Cl.

For many adsorbates on Si (including Cl), laser induced diffusion to the bulk is significant only at fluences above the surface melting threshold: the diffusion coefficient D of most impurities in solid silicon is so small that the calculated diffusion length during an excimer laser pulse is much smaller than the separation between two adjacent (100) planes; however, it is larger by seven orders of magnitude in liquid silicon with the result that the diffusion length becomes comparable to the melted depth [23], which is 130 nm at a laser fluence of 600 mJ cm^{-2} for a 20 ns laser pulse at 308 nm [9]. The diffusion coefficient for Cl in liquid Si is not known. However, its order of magnitude is the same for all elements for which it is known, so we use for Cl the average of diffusion coefficients measured for other elements: $D = 3 \times 10^{-4}$ cm^2 s^{-1} [27]. The corresponding diffusion length is $(D\tau)^{1/2} \approx 390$ Å, using the measured duration of melting $\tau \approx 50$ ns [9]. This length defines the spatial scale of the decrease of Cl concentration induced by diffusion during one single laser pulse.

The state of the substrate and adsorbate after the laser pulse depends not only on desorption and diffusion to the bulk during the laser pulse, but also on the impurity redistribution which is induced by segregation at the moving liquid–solid interface during surface recrystallization [24–30]. Segregation is related to the different solubilities of impurities in the liquid and solid phases and it also depends on the dynamics of recrystallization. It is characterized by the segregation coefficient which is defined as the ratio n_s/n_l of the concentrations in the solid and liquid phases. At equilibrium, the segregation coefficient strongly depends on the element; it increases towards unity as the interface velocity increases [28]; velocities in the range 1 to 12 m/s are obtained during nanosecond pulsed laser experiments at 308 nm, for laser fluences in the range 350–1000 mJ cm^{-2}, the upper value being close to the threshold for amorphization [27]. Despite these conditions, the segregation coefficient is not necessarily equal to unity, and segregation strongly influences the final concentration depth profile of incorporated impurities. In the case of a segregation coefficient notably lower than unity, impurity atoms are brought closer to the surface by recrystallization. A segregation coefficient very close to unity tends to induce a flat distribution of impurities over the melted depth after only a few laser pulses [27].

There have been several studies of chlorine adsorption on Si(100). Chlorine chemisorbs dissociatively. According to most studies, the surface is passivated by the adsorption of one Cl monolayer (ML) [31]. However, one work brings up the existence of a second, weakly bound, unsaturated state which was observed by temperature programmed desorption (TPD) [32]. None of our experimental observations, including Auger experiments, seems to involve such a state. If it exists, it does not seem to play a role in laser desorption experiments, perhaps because it would be emptied very quickly at the very early stage of laser heating: its reported peak is only 200°C in TPD. Therefore we ignore the possible existence of such an adsorption state. At saturation, the Si(100)2×1 reconstruction is not removed [33–35]. This is in contrast with the case of the (111) orientation for which the 7×7 reconstruction is removed by chlorine adsorption [36]. The Si(100):Cl surface structure results from the bonding of Cl electrons with the single dangling bond present on each Si atom in the 2×1 reconstruction. As a result, the Cl atoms sit obliquely on Si atoms [37]. The Si:Cl ratio is unity at saturation and 1 ML contains 6.78×10^{14} at cm^{-2}. Finally, the sticking coefficient of Cl_2 at room temperature is ~ 0.1 [5,36].

Laser etching of silicon by chlorine has been studied extensively for both the (100) and (111)

orientations. The results may be summarized as follows: (1) the laser desorption of silicon chlorides already present at the surface at the instant of the laser pulse requires surface melting [9]. (2) The reactive scattering of gas phase molecular or atomic chlorine at the silicon surface requires kinetic energy (threshold: 5 kJ/mol in the case of Cl_2 on Si(111)) [18–20]. Laser excitation (threshold: 20–40 mJ cm^{-2} in the region 355–560 nm for Si(111) [18–20]) is also necessary at thermal energies [12,14]. Reactive scattering has been observed in the absence of a laser beam for Cl_2 kinetic energies above ~ 1 eV [21]. Over a wide range of pressures (i.e. below 100 mbar), process (1) (photodesorption) dominates the etch rate [12,17], and in this paper we focus our attention on it [5–11,15,16]. Hence, we use laser fluences above the melting threshold, which is ~ 350 mJ cm^{-2} for our excimer laser at 308 nm [9]. The mechanism of photodesorption is most probably evaporation of molecules (mainly SiCl) from the laser melted surface: there is a laser fluence threshold for photodesorption which was experimentally found to coincide with the surface melting threshold [9]; the etch rate saturates at 0.56 Å/pulse (or 0.40 Si ML/pulse) [5]; the desorption yield on the solid surface is lower than 10^{-4} Si ML/pulse [9].

The aim of this work is to understand why the etch rate is limited to the value of 0.40 Si ML/pulse. We measure both desorbed SiCl molecules using time of flight (TOF) mass spectrometry, and undesorbed Cl atoms using Auger electron spectroscopy (AES) and secondary ion mass spectrometry (SIMS). This allows us to measure the amounts of undesorbed and desorbed Cl in reactive and unreactive form. Evidence of Cl diffusion to the bulk, and of strong segregation of Cl in Si, are presented. Diffusion results in bulk contamination, while segregation results in bulk cleaning. The net result of diffusion and segregation is that Cl incorporation to the bulk is below our SIMS sensitivity level. The laser allows to clean Si from Cl contamination in a few pulses, at undetectable levels by AES and SIMS. Laser cleaning of Cl, C and O are compared.

2. Experimental

Two experimental setups have been used, one with a base pressure of 10^{-7} mbar, and the other one with a base pressure of 2×10^{-10} mbar. The secondary vacuum apparatus has been described in details previously [5,9]. Briefly, a pulsed molecular beam of chlorine allows the controlled (up to 1 ML), pulsed (up to 100 Hz) dosing of a silicon sample at a static working pressure in the range 10^{-7} to 10^{-6} mbar. A "pump" laser beam (308 nm or 337 nm) produces the desorption of silicon chlorides. Laser desorbed SiCl molecules are ionized by a "probe" laser beam at a variable delay after the pump laser pulse by resonantly enhanced multiphoton absorption at 308 nm. The $SiCl^+$ ions are detected on microchannel plates after passing through a time of flight (TOF) mass spectrometer which is used as a mass selector. By varying the delay between the pump and probe lasers, the velocity distribution of desorbing SiCl molecules is measured. The SiCl desorption yield taken as the TOF SiCl peak height is calibrated against the absolute etch rate as measured ex situ with a DEKTAK surface profiler.

The UHV apparatus (Fig. 1) is equipped with a RIBER sample manipulator, a VG Monitor 100 D quadrupole mass spectrometer, an ion gun, an electron gun, and a VSW Class 100 hemispherical electron spectrometer which was used for AES. In AES experiments, we used an incident electron kinetic energy of 2000 eV at an incidence angle of 48° with respect to the surface normal; the current through the sample was 100 to 200 nA; the electron beam diameter was ~ 0.4 mm; we have found no evidence of electron induced desorption under these conditions. The laser beam has a diameter of 3 mm at the surface; the electron beam is scanned across the laser spot to probe the laser induced surface modifications. The emitted electrons are collected at 45° off the surface normal.

The undifferentiated $E\,N(E)$ spectra are used for measurements. When the electron current and energy and the sample orientation are kept constant, the Auger spectra at different positions across the surface are proportional to one another, and the background remains the same upon chlorine adsorption (this is shown in Fig. 2 for Si(111)). Therefore, we use for quantitative measurements the ratio of the Auger electron peak heights to the electron background at the peak energy. Throughout this paper, "peak height" stands for "ratio of peak height to the background". We have monitored the Si LVV

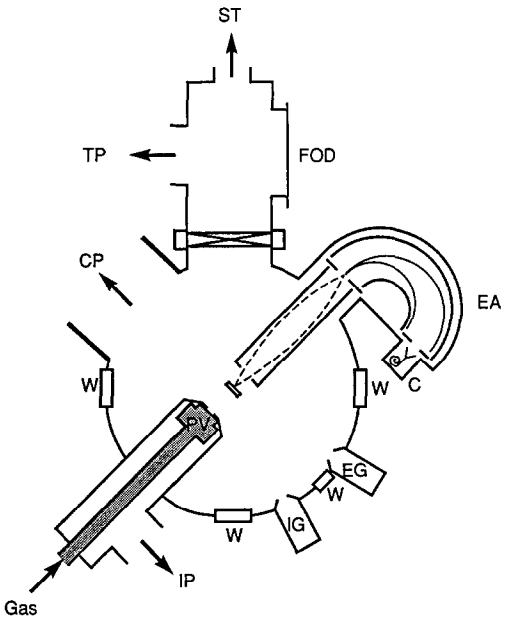

Fig. 1. Experimental UHV apparatus. The sample is on the axis of the main chamber. PV: pulsed valve. IG: ion gun. EG: electron gun. EA: electron electrostatic analyzer. C: channeltron. W: windows. IP: ion pump. CP: Cryogenic liquid He pump. TP: turbomolecular pump. ST: sample transfer. FOD: fast opening door.

and the Cl LVV Auger peaks at 92 and 181 eV, respectively. When there is no chlorine below the surface, we assume that the surface coverage is proportional to the Cl peak height. In addition, the Cl peak heights are normalized to the 1 ML peak height and are expressed in ML.

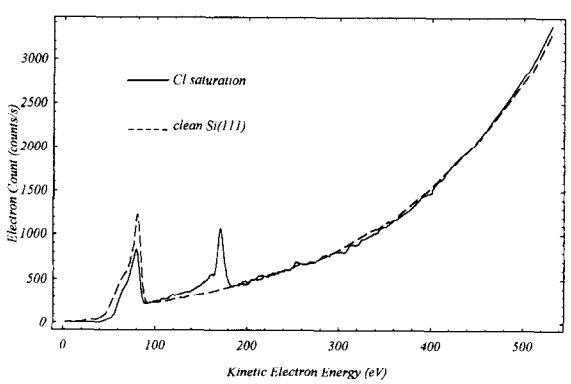

Fig. 2. AES spectra of a laser cleaned Si surface and a Cl saturated surface.

In the case where chemical changes to the Cl overlayer would be induced by the laser, the peak height might not reflect adequately the Cl coverage. Therefore we have also estimated the Cl coverages by measuring the Cl peak areas between 130 and 190 eV: the results of the two methods are comparable within 0.02 ML.

Si samples (p-type, B-doped, $\rho = 1$–$5\ \Omega \cdot$ cm) are oriented towards (100). They are prepared by the standard RCA method. In the secondary vacuum experiment, they are laser annealed (at a laser fluence of 600 mJ cm^{-2}, i.e. above the surface melting threshold, but well below the ablation threshold) for a hundred laser shots. From the background static pressure ($< 10^{-6}$ mbar for chlorine, $< 10^{-7}$ mbar for other gases), the laser repetition rate (> 10 Hz), and the sticking coefficient of Cl_2 on Si(100) (~ 0.1) [6], we estimate the surface contamination between two laser pulses to be much less than 10^{-2} ML for all contaminants. Considering that the laser pulse at the fluences used here has the effect of cleaning the surface (see below), it is reasonable to assume that the Si surface is clean from contaminants other than chlorine. For secondary vacuum experiments, 1 ML is defined as the coverage which leads to the saturation *of the etch rate* as the chlorine dose between two laser pulses is increased. With this definition, we have obtained no inconsistencies between the TOF and the AES experiments.

In the UHV experiment, two methods were used to clean the surface: argon ion erosion followed by annealing at 600°C, and laser annealing. The surface cleanliness is checked by AES. After cleaning, carbon and oxygen are not observable (Fig. 2). Efficient laser cleaning of silicon is obtained with a few hundred laser pulses at a fluence in the range 500 to 600 mJ cm^{-2}. The ratio of the Si peak height to the background is equal to ~ 4 and to ~ 8 for the sputtered and annealed samples and the laser annealed ones, respectively. Since for the sputtered and annealed samples the Si peak height increases with annealing temperature and duration, this might be considered as an indication of the good "quality" of the laser cleaned surfaces; however, it might also indicate some surface disorder. Laser cleaned Si(100) surfaces have indeed been reported to exhibit the 2×1 reconstruction, and to be slightly more disordered than thermally cleaned surfaces (900°C), based

on EELS and RHEED studies [38]. We have observed no difference between the two types of surfaces in the behavior towards chlorine. Fig. 2 shows AES spectra of the laser cleaned and Cl saturated surface.

We emphasize the fact that the fluence of 600 mJ cm^{-2} is much lower than the damage threshold of ~ 1 J cm^{-2}. At such a fluence, the surface is severely roughened after $\sim$ one hundred pulses, as evidenced by the fact that it becomes dark, and as revealed by the profiler. At fluences of ~ 600 mJ cm^{-2}, and if the number of laser pulses is more than about one hundred, a careful examination of the surface by eye reveals the contour of the illuminated spots. No other anomaly is observed. This visible contour may be due to stuctural defects induced by the thermal shocks at the boundary of the laser beam. The temperature rise is as large as ~ 1400 K in ~ 10 ns and ~ 1 μm. The cooling is not as fast, but its time and space scales are still very short (a few 100 ns and a few μm, respectively).

A SIMS apparatus (Cameca SMI 300) is used ex situ for measuring the Cl depth profile after laser etching by 20 to 2800 laser pulses. The sample is sputtered by O_2^+ primary ions of 5.5 keV at a current of 100 nA. The ion beam has a diameter of 100 μm on the surface. The sputtered area has a diameter of 600 μm. The secondary ions are analysed by means of a single magnetic field and counted. The SIMS sputtered depth is systematically calibrated with a DEKTAK profilometer. Possible variations of the sputtering rate with the Cl concentration was not investigated. However, considering the very low Cl concentrations achieved in this work, Cl induced variations of the sputtering rate are improbable. Under our experimental conditions, the O signal stabilizes after sputtering of a depth of ~ 25 nm (this stabilization corresponds to the equilibration of O incorporation and sputtering rates during analysis).

3. Results

3.1. Variations of the state of the substrate with the type of experiment (TOF, SIMS AES)

In this paper, we discuss TOF, SIMS and AES measurements corresponding to an initial surface coverage of 1 ML and to a laser fluence of 600 mJ cm^{-2}. The chlorinated silicon before the laser pulse is not identical in all types of experiments. For TOF experiments, the data are accumulated over a series of $2^{14} = 16384$ laser pulses. Each measurement consists in a single exposure to chlorine followed by a series of $\mathcal{N}$ laser pulses ($\mathcal{N} = 1$ to 8), depending on the experiment. Therefore, before the first laser pulse of the series, there is a Cl monolayer at the surface and possibly Cl in the bulk which has diffused below the surface in the course of previous measurements. In AES experiments, an atomically clean Si sample is exposed to a controlled chlorine dose. As a result, the bulk is clean. The sample is exposed to one single laser shot and Auger spectra are then recorded. In the case of readsorption experiments, it may be contaminated by Cl diffusion induced by a known small number of laser pulses. Therefore, the comparison between TOF and AES experiments requires to estimate the influence of bulk Cl on desorption and diffusion. The SIMS measurements reported here were done on samples etched in our TOF apparatus.

3.2. Notations

In both experiments, the initial surface and bulk Cl are redistributed by the effect of the laser pulse into the gas phase, the surface and the bulk:

$$D_{\mathrm{des}} + \theta_0 + D_{\mathrm{dif}} = \theta_0^0 + D_{\mathrm{dif}}^0, \tag{1}$$

where D_{des} and D_{dif} are the amounts of desorbed and diffused Cl atoms per unit area, respectively, D_{dif}^0 is the initial amount per unit area of Cl in the layer to be melted by the laser, θ_0^0 and θ_0 are the initial and final surface coverages, respectively. For atomically clean bulk and Cl saturated surface, $\theta_0^0 =$ 1 ML and $D_{\mathrm{dif}}^0 = 0$. In TOF experiments, D_{dif}^0 is generally not zero. Its actual value may depend strongly on $\mathcal{N}$. It will be shown below that $D_{\mathrm{dif}}^0 \approx 0$ for $\mathcal{N} = 8$. D_{des}, D_{dif} and D_{dif}^0 may be expressed in ML. After recrystallization, the undesorbed atoms may be distributed in the whole melted layer:

$$D_{\mathrm{dif}} = \sum_{i=1}^{N} \theta_i, \tag{2}$$

where N is the number of (100) planes in the melted layer, and θ_i the Cl content of the Si plane number i after recrystallization.

AES probes only a thin surface layer. We arbitrarily define its thickness as the depth corresponding to an attenuation of Cl Auger electrons at 181 eV of 10^{-1}. The mean free path of electrons of 181 eV energy is 2 to 5 atomic planes [42]. This corresponds to a transmission factor of electrons by one single atomic plane of $\alpha = 0.71 \pm 0.11$. With this transmission factor, the contribution of an atom in the 7th atomic plane is 0.09 times that of a surface atom, so our "AES layer" corresponds to the first seven Si planes. The spatial scale of diffusion (as estimated in the introduction section) is ~ 1 order of magnitude larger than the AES depth. Therefore, AES measurements only allow to estimate θ_0 and D_{AES}, the fraction of Cl atoms which are found in the AES layer after the laser pulse. Atoms that diffuse to deeper planes can be probed by SIMS:

$$D_{dif} = D_{AES} + D_{SIMS}, \tag{3}$$

$$D_{AES} = \sum_{i=1}^{7} \theta_i, \tag{4}$$

$$D_{SIMS} = \sum_{i=8}^{N} \theta_i. \tag{5}$$

The AES signal I_{AES} is not proportional to D_{AES}, because the contribution of each plane has a different attenuation factor. Assuming that Cl atoms produce the same attenuation on 181 eV electrons as Si atoms, the AES signal I_{AES} is equal to

$$I_{AES} = \theta_0 + (1 - \theta_0 + \alpha\theta_0) \sum_{i=1}^{N} \alpha^{i-1}\theta_i, \tag{6}$$

which can be rewritten as

$$I_{AES} = \theta_0 + (1 - \theta_0 + \alpha\theta_0)\mathcal{J}, \tag{7}$$

with the definition

$$\mathcal{J} = \sum_{i=1}^{N} \alpha^{i-1}\theta_i. \tag{8}$$

Chlorine may desorb in various forms, reactive and unreactive, so D_{des} is equal to

$$D_{des} = D_{react} + D_{unreact} = (D_{SiCl} + 2\ D_{SiCl_2}) + (D_{Cl} + 2\ D_{Cl_2}), \tag{9}$$

where D_X is the amount of desorbed X molecules per unit area. For Si atoms, the desorption yield D_{Si} is equal to

$$D_{Si} = D_{SiCl} + D_{SiCl_2}. \tag{10}$$

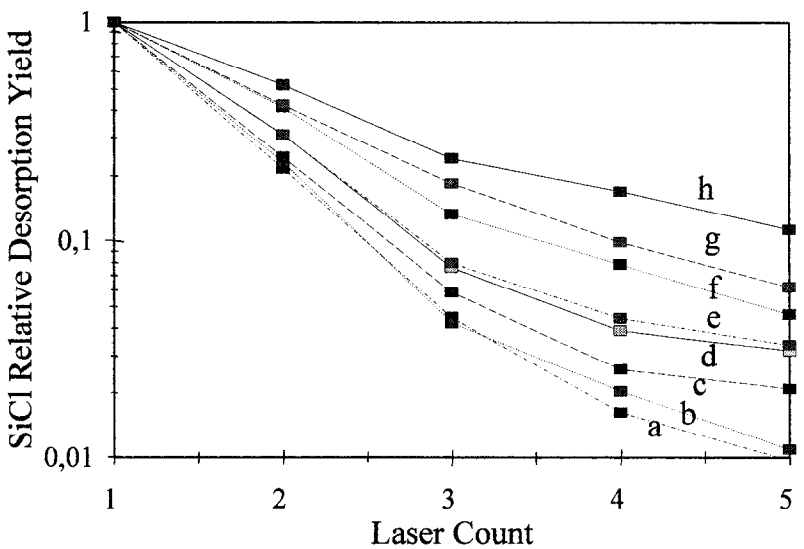

Fig. 3. Relative desorption yield of SiCl in a series of laser pulses following one single chlorine dose (TOF measurements with laser ionization of desorbed SiCl). Several values of the chlorine dose have been used, resulting in an absolute Si desorption yield at the first pulse of (a) 4.0×10^{-1}, (b) 9.1×10^{-2}, (c) 3.7×10^{-2}, (d) 4.6×10^{-3}, (e) 3.0×10^{-3}, (f) 4.1×10^{-4}, (g) 1.6×10^{-4}, (h) 4.7×10^{-5} ML.

In what follows, we estimate the values of D_{des}, D_{dif}, and θ_0. One difficulty arises from the fact that these quantities are not directly measured with the techniques used here. D_{Si} is measured absolutely. D_{SiCl} is measured only relatively by TOF, as a function of laser pulse count. The ratio between D_{SiCl} and D_{SiCl2} can only be roughly estimated by TOF.

We shall first show the experimental results. The estimations of D_{AES}, D_{SIMS}, D_{des} and D^0_{dif} will be presented in the next section.

3.3. TOF results

The etch rate D_{Si} exhibits a saturation at 0.40 ML/pulse above the fluence of ~ 500 mJ cm^{-2} [9]. In order to investigate the origin of this saturation, we have monitored the desorption of SiCl molecules in a series of $\mathcal{N}$ laser pulses following one single exposure to chlorine. The fluence was 600 mJ cm^{-2}, which is in the saturation range. *The desorption yield after the first pulse does not fall to zero*, showing that the saturation does not correspond to the desorption of all chlorine. It decreases with laser count i (Fig. 3). It falls by nearly three orders of magnitude between $i = 1$ and $i = 8$, but it is still measurable after 8 pulses. The experiment was performed for various initial surface coverages in the range between 1 ML ("a" in Fig. 3) and $\sim 10^{-4}$ ML ("h" on Fig. 3).

The absolute etch rate per Cl pulse D_{Si} ($\mathcal{N}$) is measured with the depth profiler (Table 1). We scale the relative SiCl desorption yield D_{SiCl} (i) at pulse i so that D_{Si} ($\mathcal{N}$) $= \sum_{i=1}^{\mathcal{N}} D_{SiCl}$ (i). The results are shown in Table 1 for $\mathcal{N} = 1$–3. We find that the SiCl desorption yield at the first pulse does not vary with $\mathcal{N}$ by more than 10%, which is of the order of magnitude of the experimental uncertainty. This result suggests that the presence of Cl in the bulk has a small effect on the desorption yield: after the Cl

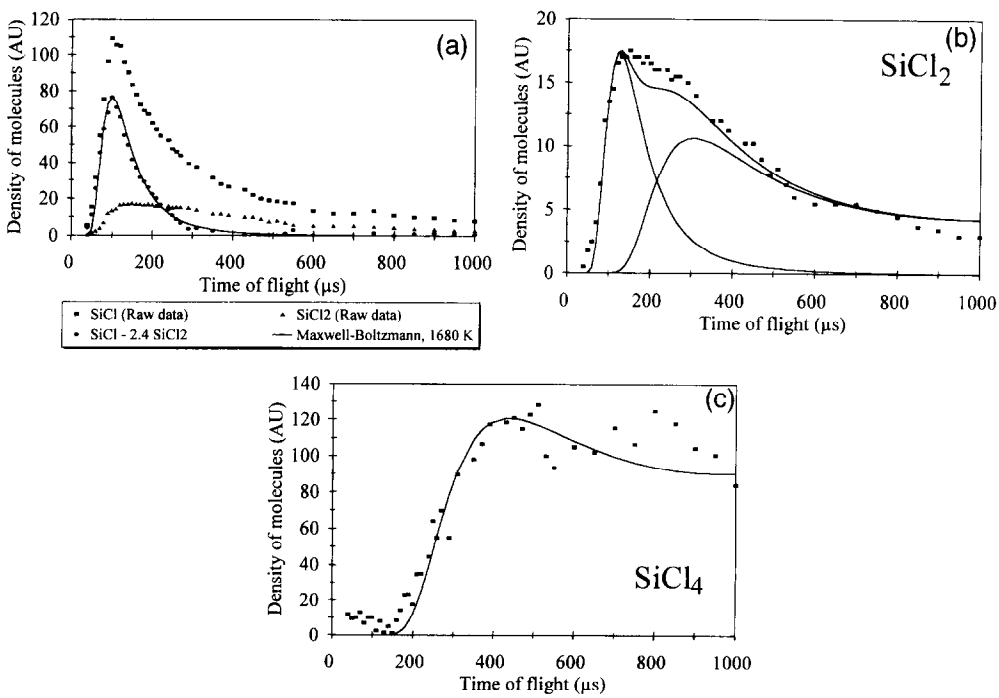

Fig. 4. (a) Experimental TOF spectra of laser desorbed SiCl and $SiCl_2$. The ionization is by electron impact. The estimated contribution of $SiCl_2$ cracking to SiCl is subtracted from the SiCl distribution. The resulting SiCl distribution is fitted to a Maxwell–Boltzmann distribution at 1680 K. (b) Experimental TOF spectrum of $SiCl_2$. The data are modelled by the sum of a Maxwell–Boltzmann distribution at 1680 K, and a phenomenological distribution corresponding to wall reactions (see text). (c) Experimental TOF spectrum of $SiCl_4$. The data are entirely assigned to wall reactions, and are modelled by the same phenomenological distribution as for $SiCl_2$ (see text).

Table 1
Absolute desorption yield of Si (D_{Si} ($\mathcal{N}$), as measured with the depth profiler) as a function of $\mathcal{N}$, the number of laser pulses between two Cl pulses, and (below separator) relative desorption yield of SiCl (D_{SiCl}, as measured by TOF) as a function of laser count i for $\mathcal{N} = 8$

$\mathcal{N}$, number of laser pulses between 2 Cl pulses	1	2	3
D_{Si} ($\mathcal{N}$), etch rate per Cl pulse (ML/pulse)	0.40	0.52	0.55
D_{SiCl} (1), SiCl desorption yield at the 1st laser pulse	0.40	0.43	0.44
D_{SiCl} (2), SiCl desorption yield at the 2nd laser pulse		0.09	0.09
D_{SiCl} (3), SiCl desorption yield at the 3rd laser pulse			0.02
Total (SiCl desorption yield for one Cl pulse)	0.40	0.52	0.55

Experiments consist of one Cl pulse followed by $\mathcal{N}$ laser pulses. The TOF measurements are scaled so that $D_{Si}(\mathcal{N}) = \sum_{i=1}^{\mathcal{N}} D_{SiCl}(i)$. The laser fluence is 600 mJ cm^{-2}.

pulse and before the first of the $\mathcal{N}$ laser pulses, the Cl surface coverage (which results from resaturation of the surface by the Cl pulse) does not depend on $\mathcal{N}$, so the contribution of surface Cl to the desorption yield sould be constant with $\mathcal{N}$. On the other hand, we expect the bulk to be cleaner as $\mathcal{N}$ increases. So the contribution of bulk Cl to the desorption yield should decrease with $\mathcal{N}$. No such decrease is observed experimentally. The SiCl desorption yield, which strongly depends on surface coverage [5], depends little on the possible presence of Cl below the surface. This may mean that there is in fact no significant amount of Cl just below the surface. Alternatively, the small effect of bulk Cl on desorption may be related to the rather large Cl concentration gradient at the beginning of the laser pulse: the Cl atoms located just below the surface would be repelled by surface atoms towards the bulk.

The branching ratio between SiCl and $SiCl_2$ may be estimated from previous TOF measurements from our group [6]. In these measurements, ionization of the desorbed molecules was by electron impact. There are three difficulties in estimating the $SiCl/SiCl_2$ ratio from the integrated velocity distributions of both molecules (Fig. 4). One is that the relative ionization efficiencies of SiCl and $SiCl_2$ are not known. We assume in what follows that they are equal: for both molecules, ionization consists in removing one electron from the Si atom. The assumption is that the details of the electronic structure of both molecules and molecular ions do not affect too much the ionization efficiency. While this assumption is not valid for ionization at a well defined energy (as is the case for laser ionization), it may be used for the broad distribution of electron energies in our ionization source.

The second difficulty comes from the cracking of $SiCl_2$ upon ionization. Some experimental information is available. Li et al. [18,19] have reported velocity distributions of SiCl and $SiCl_2$ molecules desorbed from Si(111) under conditions different from ours, where $SiCl_2$ is the only desorption product. As a result, SiCl has the same velocity distribution as $SiCl_2$ in Refs. [18,19], while SiCl and $SiCl_2$ have different velocity distributions in our experiment [6]. The $SiCl/SiCl_2$ ratio is ~ 2 in Li's paper, and this ratio directly reflects the cracking pattern of $SiCl_2$. Matsuo et al. [44] also reported TOF spectra of SiCl and $SiCl_2$ under conditions of thermal desorption from Si(111), where SiCl is not desorbed. Their measurement of the $SiCl/SiCl_2$ ratio is ~ 3.4. In our experiment, $SiCl_2$ has a longer flight time than SiCl, so we may assume that the tail of the SiCl TOF spectrum is entirely due to cracked $SiCl_2$: this yields a $SiCl/SiCl_2$ cracking ratio of 2.4 ± 0.4. Since this value is in reasonable agreement with the one of Li et al., and not too different from that of Matsuo et al., we use it in what follows.

The third difficulty arises from wall reactions. As is evident from Fig. 4, neither the SiCl nor the $SiCl_2$ TOF spectra have a Maxwell–Boltzmann (MB) shape. Their rising edges do correspond to a MB at 1680 K, but in both cases there is a second, slower component, that extends to much longer times than the MB distribution. In the case of SiCl, the difference between the raw SiCl data and the $SiCl_2$ data (multiplied by the cracking coefficient of 2.4) can be readily fitted to a MB distribution at 1680 K (Fig. 4a), suggesting strongly that the long tail of SiCl is in fact due to the cracking of $SiCl_2$. The second component of $SiCl_2$ is assigned to reactions on the walls of the mass spectrometer. Wall reactions were shown to occur after the present measurements were performed; by placing a diaphragm at the entrance of the spectrometer, the tail of the SiCl spectrum disappeared [11]. The wall reactions are also evidenced by

the presence of some $SiCl_4$ in the mass spectrum. The rising edge of the $SiCl_4$ TOF spectrum corresponds to exceedingly slow $SiCl_4$ which cannot be assigned to laser desorption (Fig. 4c). Both the $SiCl_4$ spectrum, and the $SiCl_2$ spectrum obtained by difference between the $SiCl_2$ raw data and a MB distribution at 1680 K, can be modelled by a same function. In the range of time of flight displayed in Fig. 4, this function is arbitrarily chosen as a convolution of a MB distribution (with a fitted temperature of 390 K) with the exponential term $\exp(t/t_0)$ with $t_0 = 275$ μs (Figs. 4b and 4c). The exponential reflects the delay of the wall reactions with respect to the laser pulse.

The actual ratio of desorbed SiCl to $SiCl_2$ is estimated from the integration of the two MB distributions of Figs. 4a and 4b (after conversion of the data from densities to fluxes). The integral of $SiCl_2$ must be multiplied by 3.4 ± 0.4 to account for $SiCl_2$ cracking. The result is that the ratio of SiCl to $SiCl_2$ is 1.3 ± 0.3. Thus SiCl is at least as abundant as $SiCl_2$ in the desorption products. From this and from the value of the etch rate $D_{Si} = 0.40 \pm 0.03$ ML obtained from profilometer measurements, Eqs. (9) and (10) yield (Table 2):

$$D_{SiCl} = 0.23 \pm 0.04 \text{ ML},$$

$$D_{SiCl_2} = 0.17 \pm 0.04 \text{ ML},$$

$$D_{react} = 0.58 \pm 0.07 \text{ ML}.$$

A question relative to the $SiCl/SiCl_2$ ratio is whether it depends on experimental conditions that might influence the surface chemistry, such as laser fluence and the number $\mathcal{N}$ of laser pulses between Cl pulses. Since we do not measure routinely $SiCl_2$, the proportionality of D_{Si} and D_{SiCl} is our means to check that the ratio of SiCl and $SiCl_2$ desorption yields remains constant. We have reported previously that D_{Si} and D_{SiCl} remain proportional to each other over one order of magnitude of D_{Si} when the laser fluence is changed [10]. For experiments with $\mathcal{N} > 1$ ($\mathcal{N}$ laser pulses following every Cl pulse), the SiCl desorption yield at the first pulse following the Cl pulse, D_{SiCl} (1), does not vary with $\mathcal{N}$ by more than 10%, which is approximately the experimental uncertainty (Table 1). A change of 10% in D_{SiCl} for a fixed D_{Si} corresponds to a larger relative change of the $SiCl/SiCl_2$ ratio, but the ratio remains within experimental uncertainty: there is no evidence of a variation of the etch rate, or of the $SiCl/SiCl_2$ ratio, as the laser fluence or $\mathcal{N}$ are changed.

Table 2
Branching ratios for desorption and diffusion induced by one single laser pulse, of 1 Cl ML adsorbed on atomically clean Si(100)

	Branching ratios (ML/pulse)
Si desorption ($SiCl + SiCl_2$)	$D_{Si} = 0.40 \pm 0.03$
Cl reactive desorption ($SiCl + 2SiCl_2$)	$D_{react} = 0.58 \pm 0.07$
Cl unreactive desorption ($Cl + 2Cl_2$)	$D_{unreact} = 0.12 \pm 0.07$
Cl in the "AES layer" (planes 0 to 7)	$D_{AES} = 0.37 \pm 0.13$
Cl in the "SIMS" layer (planes 8 to 950)	$D_{SIMS} = 0.10 \pm 0.10$
Sum	1.17 ± 0.37

The laser fluence is 600 mJ cm^{-2}. SiCl and $SiCl_2$ are assumed to have the same ionization efficiency, and the cracking of $SiCl_2$ is estimated to yield a SiCl to $SiCl_2$ ratio of 2.4 ± 0.4. The Si desorption yield (as measured with a Dektak profilometer) is also indicated for comparison. The desorbed amount is estimated from depth profiler and TOF measurements. The amount present in the "AES layer" is estimated from AES measurements. The amount of Cl located in the "SIMS layer" is estimated from SIMS measurements. The measured SiCl to $SiCl_2$ ratio during laser desorption is 1.3 ± 0.3. It is assumed that the desorption yields of SiCl, $SiCl_2$, Cl and Cl_2 do not vary with laser count. The sum should be 1 ML.

3.4. SIMS results

A typical Cl depth profile obtained by measuring the sputtering rate of $^{35}Cl^-$ secondary ions on a sample area that was previously etched by 2000 laser pulses is displayed in Fig. 5. Cl profiles exhibit a narrow surface peak of width at half maximum ~ 2.5 nm for any number of laser pulses in the range 20–2000. Because the samples are exposed to air before SIMS analysis, the surface peak may be related to surface contamination. The height of the surface peak ranges from ~ 7 to $\sim 3 \times 10^{20}$ cm^{-3}, *decreasing* with laser pulse number between 200 and 2000 (our measurement for 20 pulses is not directly comparable in intensity to the other measurements). Therefore, there is no indication of Cl

accumulation near the surface during laser etching. The corresponding peak area ranges from ~ 1.3 to $\sim 3 \times 10^{14}$ cm^{-2}. This is equivalent to a coverage of a few tenths of a monolayer, which is a reasonable order of magnitude by comparison with the initial 1 ML.

Sample areas that were only exposed to chlorine (and not to the laser), exhibit a surface peak which is $\sim$ twice broader and $\sim$ twice larger than areas etched by the laser. We would rather expect the non-etched areas to have only 1 Cl ML at the surface (because Cl chemisorption passivates silicon), while the etched areas should have 1 Cl ML at the surface (due to the adsorption of residual chlorine gas after laser processing) and possibly some Cl in the bulk. On the other hand, laser etched areas are cleaned by means of the laser before etching, which is not the case for non-etched areas. We conclude that at least on non-etched areas, the surface peak contains impurities from the background due to other masses. In any case, there is definitely no accumulation of Cl near the surface induced by laser etching.

At depths beyond the surface peak, the Cl density falls below the detection sensitivity of Cl in our SIMS apparatus, which is estimated to be $\sim 10^{19}$ cm^{-3}, from our signal of Si^- and from tabulated sensitivities of SIMS for Si^- and Cl^- [43]. The content in each Si plane corresponding to 10^{19} cm^{-3} is 2×10^{-4} ML. The melted depth of 130 nm at 600 mJ cm^{-2} corresponds to ~ 950 Si(100) planes, so the upper limit for D_{SIMS} (neglecting the surface peak) is 0.19 ML. We conclude that $D_{SIMS} = 0.10 \pm 0.10$ ML (Table 2).

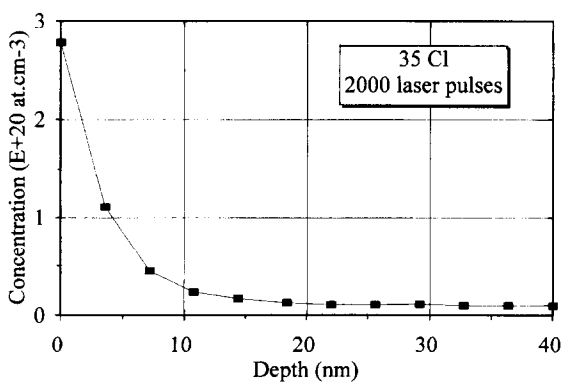

Fig. 5. ^{35}Cl depth profile measured by SIMS on a spot that was previously etched by 2000 laser pulses at a fluence of 600 mJ cm^{-2}.

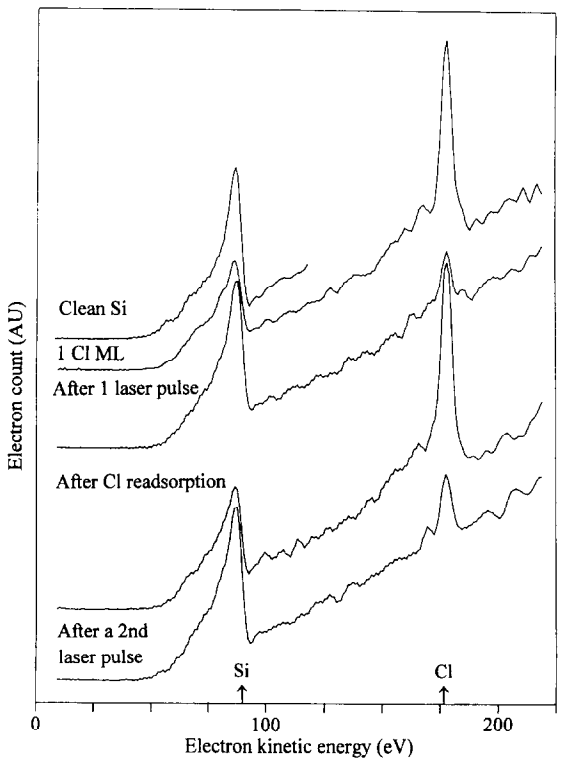

Fig. 6. AES spectra after: laser cleaning, chlorine saturation, one laser pulse, chlorine resaturation and a second laser pulse. I_1 and I_2 (see text) are the chlorine peak heights after one laser pulse and after chlorine resaturation, respectively.

3.5. AES results

A typical set of AES experiments is shown in Fig. 6 for the same laser fluence as for TOF experiments (600 mJ cm^{-2}). The spectra were recorded after: surface cleaning, Cl saturation, one laser pulse, Cl resaturation and one additional laser pulse. As may be seen in Fig. 6, Cl is still observed after one laser pulse, with a peak height $I_1 = 0.29 \pm 0.03$ ML. Resaturation of the surface by chlorine yields an Auger signal which is marginally (but reproducibly) larger than the monolayer signal, $I_2 = 1.05 \pm 0.03$ ML.

According to Eq. (7), the AES intensities I_1 (after one pulse) and I_2 (after rechlorination) can be expressed as

$$I_1 = \theta_0 + (1 - \theta_0 + \alpha\theta_0)\mathcal{J}, \quad (11)$$

$$I_2 = 1 + \alpha\mathcal{J}. \quad (12)$$

Therefore, $\mathcal{J}$ can be calculated from I_2:

$$\mathcal{J} = \frac{I_2 - 1}{\alpha}, \tag{13}$$

and the surface coverage θ_0 can be expressed as a function of I_1 and I_2:

$$\theta_0 = \frac{I_1 - (I_2 - 1)/\alpha}{1 - (1 - \alpha)(I_2 - 1)/\alpha}. \tag{14}$$

The experimental values yield

$\theta_0 = 0.22 \pm 0.10$ ML,

$\mathcal{J} = 0.07 \pm 0.05$ ML.

The large uncertainties on θ_0 and $\mathcal{J}$ are due to the fact that the bulk signal is at the limit of sensitivity of AES, and also to the large uncertainty on α. Let us note that they are *not* independent. These results provide direct evidence that a non negligible fraction of Cl atoms are not desorbed by the laser. In addition, the fact that much Cl is found *at* the surface shows that there is segregation of Cl at the Si liquid/solid interface. A value of D_{AES} can be extracted from θ_0 and $\mathcal{J}$, based on a model of the dependence of θ_i on i. This will be discussed in Section 4.

Fig. 7 shows the AES signal as a function of laser count. Cl resaturation of the surface was done between pulses 1 and 2. The signal after the second laser pulse shows a small effect of Cl accumulation: for this pulse, there was initially Cl below the surface (D^0_{dif} was not zero), which explains that the AES signal is larger than after the first laser pulse, for which D^0_{dif} was zero. The AES signal decreases quickly with laser count. It falls below the AES sensitivity level (~ 0.01 ML) after the 4th laser pulse.

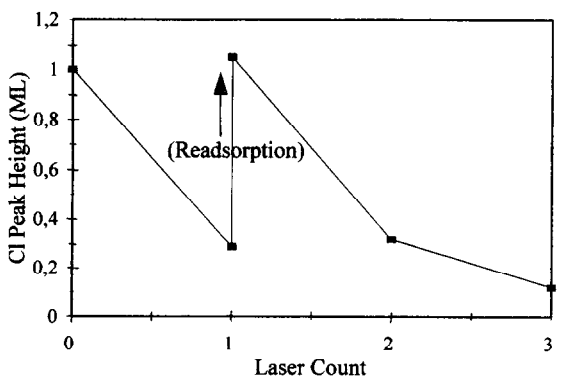

Fig. 7. Laser induced desorption of Cl as probed by AES as a function of laser count. The surface was rechlorinated (with no cleaning) after the first laser pulse. The laser fluence is 600 mJ cm^{-2}.

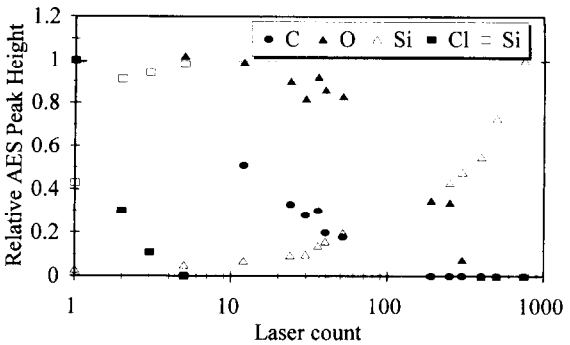

Fig. 8. AES peak heights of Cl, C, O and Si as a function of laser count during laser cleaning at 600 mJ cm^{-2}. The peak heights are normalized to the initial value (contaminated surface) for impurities (Cl, C and O), and to the final value (clean surface) for Si. Two sets of data are displayed: one corresponding to the cleaning of 1 Cl ML (squares) and one corresponding to the cleaning of Si after baking the vacuum chamber (circles and triangles).

Fig. 8 compares the efficiencies of laser cleaning of Si from Cl, C and O impurities. However, the initial state of the surface is different for Cl measurements on the one hand, and for C, O and Si on the other hand. The initial state is 1 Cl ML on an atomically clean substrate in the case of Cl. By contrast, the initial state is undefined in the case of the C, O and Si measurements: the substrate is cleaned chemically ex situ and introduced in the chamber which is subsequently baked at ~ 250°C for 24 h. In the Auger spectrum, the Si peak is originally weak, and exhibits the shoulder characteristic of SiO_2. We conclude that the order of magnitude of C and O coverages is a few ML. This difference in the initial contaminated state reflects in fact the different natures of Cl adsorption with respect to C and O adsorption: Cl passivates Si, while C and O may be easily incorporated in Si. With this difference, the efficiency of laser cleaning is clearly Cl > C > O. It takes typically 5, 100 and 500 laser pulses to remove Cl, C and O respectively, at the sensitivity of AES. Interestingly, the order of efficiency for C and O is inverted with respect to ion sputtering cleaning. Ion sputtering removes O more

efficiently than C. C is removed by the laser in typically one second with the excimer laser operated at 100 Hz.

4. Discussion

4.1. Evidence for Cl diffusion to the bulk

If the laser induced desorption mechanism was just evaporation from the melted surface, the desorption yield per laser pulse would increase with laser fluence until all chlorinated molecules are desorbed during the pulse. A saturation of the desorption yield with laser fluence is indeed observed at ~ 500 mJ cm^{-2} [5]. However, as shown in the previous section, this saturation does not correspond to the desorption of all Cl species.

The presence of Cl on the surface after the laser pulse under the saturation regime could be due to the redeposition of SiCl molecules. Redeposition may be induced by post-desorption collisions between desorbing molecules. These collisions also affect the velocity distribution of the desorbing molecules. In a previous work, we have determined experimentally the coverage under which the TOF spectrum of desorbing molecules becomes independent of the initial coverage [11]. This coverage was found to be $\approx 10^{-2}$ ML, and this value is consistent with the expectation that the average number of post-desorption collisions per desorbing molecule decreases quickly to zero below 10^{-2} ML [39]. We conclude that no redeposition may take place below 10^{-2} ML. In this coverage range ("e" to "h" on Fig. 3), the desorption yield at pulses $i \geqslant 2$ is not equal to zero. (Relative to pulse 1, the desorption yield at laser pulse $i \geqslant 2$ is actually larger for lower initial coverage (Fig. 3).) This is evidence that part of the chlorine atoms diffuse into the substrate during surface melting, which prevents them from desorbing. AES results confirm the presence of at least 0.29 ± 0.05 Cl ML on the substrate at, or in the immediate vicinity of the surface.

4.2. Segregation of chlorine in silicon

The large value of the surface coverage $\theta_0 = 0.22 \pm 0.13$ ML after the laser pulse shows that the Cl depth profile cannot be flat: the Cl dose in the substrate would excess by far the initial 1 ML of chemisorbed Cl. So there is segregation of chlorine in silicon. The Cl content θ_i must decrease from θ_0 down to significantly lower values in a few atomic layers, as will be shown quantitatively below. This is consistent with the SIMS measurements which do not allow to detect any Cl in the bulk. The order of magnitude of the SIMS surface peak evaluated in ML is consistent with the AES signal in ML, so we may assume safely that the SIMS width of the surface peak is limited by the depth resolution of the SIMS. It is possible to be more quantitative and to set limits on D_{AES}, based on various possible models of the Cl depth profile in the AES layer (Table 3, Fig. 9). We consider the following three models for the Cl depth profile:

Table 3
Cl dose in the AES layer (D_{AES}) for several models of the Cl depth profile (see text and Fig. 9), after one laser pulse of 600 mJ cm^{-2}; the surface is initially saturated with 1 Cl ML, with the bulk atomically clean ($\theta_0^0 = 1$ ML and $D_{dif}^0 = 0$)

Model	Cl depth profile	D_{AES}
No segregation	$\theta_{i \geqslant 0} = 0.22 \pm 0.10$ ML	1.76 ± 0.80 ML (not compatible with experiment)
Intermediate segregation	$\theta_0 = 0.22 \pm 0.10$ ML $\theta_{i \geqslant 1} = 0.022 \pm 0.022$ ML	0.37 ± 0.13 ML
Strongest segregation	$\theta_0 = 0.22 \pm 0.10$ ML $\theta_1 = 0.07 \pm 0.05$ ML $\theta_{i \geqslant 2} = 0$	0.29 ± 0.05 ML

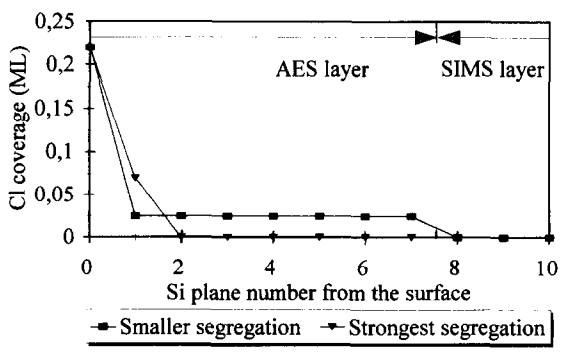

Fig. 9. Models of the Cl depth profile in the AES layer taking into account, and compatible with, AES experiments. The width of the AES layer is taken arbitrarily (see text). The Cl "coverage" in the planes of the SIMS layer is the experimental upper limit of 2×10^{-4} ML, as estimated from the SIMS measurements.

1st model: no segregation. No segregation would result in a coverage $\theta_i = \theta_0$ for all values of i. Eq. (8) would yield:

$$\mathscr{J} = \theta_0 \sum_{i=1}^{N} \alpha^{i-1} \approx \theta_0 \sum_{i=1}^{\infty} \alpha^{i-1}$$

$$= \frac{\theta_0}{1-\alpha} \approx 3.45 \times \theta_0. \qquad (15)$$

The values measured for θ_0 and $\mathscr{J}$ are not compatible with Eq. (15), the upper limit of the experimental value being $\mathscr{J}/\theta_0 = 1.00$. Hence, the θ_i for $i > 0$ must be lower than θ_0, which can only result from a segregation of Cl at the Si liquid/solid interface.

2nd model: intermediate segregation. In this model, we assume that the Cl depth profile in the AES layer is flat, except for the surface peak: $\theta_0 = 0.22 \pm 0.10$ ML (as measured). Similarly to the case of Eq. (15), Eq. (8) yields:

$$\theta_i = \frac{\mathscr{J}}{\sum_{i=1}^{7} \alpha^{i-1}} = 0.022 \pm 0.016 \text{ ML}. \qquad (16)$$

It results that in this model $D_{AES} = \theta_0 + 7\,\theta_i = 0.37 \pm 0.13$ ML (taking into account that the uncertainties on θ_0 and θ_i are not independent).

3rd model: strongest segregation. The Cl depth profile corresponding to the strongest segregation compatible with experiment is $\theta_0 = 0.22 \pm 0.10$ and $\theta_i = 0$ for $i \geqslant 2$. It then results from Eq. (8) that $\theta_1 = \mathscr{J} = 0.07 \pm 0.05$ ML. This yields $D_{AES} = \theta_0 + \theta_1 = 0.29 \pm 0.05$ ML (again, taking into account that the uncertainties on θ_0 and θ_1 are not independent).

The value $D_{AES} = 0.37 \pm 0.13$ ML takes into account the experimental uncertainties of models 2 and 3 of the Cl depth profile (Table 2). This estimation of D_{AES}, together with the SIMS upper limit on θ_i for $i > 7$, shows a very strong segregation effect for Cl in Si (Fig. 9). Segregation for Cl and C are compared in Section 4.5. Because the depth profile depends in a complicated way of the kinetics of melting, diffusion and segregation, a numerical value of the segregation coefficient cannot be obtained without computer simulation, and this was beyond the scope of this study.

4.3. Permanent regime in TOF experiments

As shown by SIMS, there is no measurable effect of Cl accumulation in the bulk over many laser pulses, although the surface is resaturated with Cl at each laser pulse: this shows that the Cl concentration in the melted layer quickly reaches its saturation value. This is not unrealistic: incorporation of only 0.01 ML at each laser pulse would result in a concentration of 10^{19} cm^{-3} in the melted layer in only 14 laser pulses, while more than $D_{AES} = 0.38 \pm 0.14$ ML diffuse into the substrate during one laser pulse. Dopant atoms also reach quickly their saturation concentration in laser doping experiments [41]. A permanent regime is quickly established. In that regime, the amount of Cl adsorbed between two laser pulses, $1 - \theta_0$, is equal to the amount of Cl desorbed during one pulse, D_{des}. However, $1 - \theta_0$ is not known for TOF experiments.

4.4. What fraction of Cl desorbs?

We have no direct experimental information on the relative desorption yields from a clean substrate with 1 Cl ML adsorbed on it. However, after 8 laser pulses, the bulk is not far from being clean: the AES experiments show that the Cl surface coverage is below the sensitivity level of 10^{-2} ML, and TOF measurements show that the SiCl desorption yield is lower than 10^{-3} ML. Therefore, the desorption yield at the first pulse for $\mathscr{N} = 8$ yields a good approximation of the yield for the case of clean bulk. As shown previously, it appears that this yield is not significantly different from the yield at $\mathscr{N} = 1$.

$D_{unreact}$ can be estimated from D_{react} and from the profilometer measurements of D_{Si} ($\mathscr{N}$) of Table 1, using the assumption (which is verified within 10% for $\mathscr{N} = 3$) that the $SiCl/SiCl_2$ branching ratio does not vary with laser count. The D_{SiCl} measured for $i = 4$ to 8 (Fig. 3) show that no more than 0.02 ML desorb during pulses 4 to 8. Therefore, $D_{Si}(8) = D_{Si}(3) + 0.02$ ML $= 0.57 \pm 0.04$ ML. If we assume that the amount of Cl in the bulk is negligible after the 8 pulses, as Auger experiments suggest, then Eqs. (1) and (9) yield:

$$\sum_{i=1}^{8} D_{react} + \sum_{i=1}^{8} D_{unreact} = 1 \text{ ML}.$$

$\sum_{i=1}^{8} D_{\text{react}} = 0.83$ ML, from $D_{\text{Si}}(\mathcal{N} = 8) = 0.57$ ML and the $SiCl/SiCl_2$ ratio of 1.3. It follows that: $\sum_{i=1}^{8} D_{\text{unreact}} = 0.17 \pm 0.10$ ML. This is an upper limit of D_{unreact} at the first pulse. If we make the additional assumption that the reactive and unreactive desorption yields remain in the same ratio whatever the condition of the surface, we obtain $D_{\text{unreact}} = 0.12 \pm 0.07$ ML for the first pulse (clean surface).

The three independent estimations of Cl reactive and unreactive desorption, Cl in the AES layer, and Cl in the SIMS layer are reported in Table 2. There is no inconsistency between them.

4.5. Laser cleaning

The strong segregation of Cl at the Si liquid/solid interface has the practical consequence that Cl/Si is a good case for laser cleaning. Even starting from one Cl ML at the surface, the bulk remains "clean" (at the sensitivity of SIMS). In AES experiments, when more laser pulses at 600 mJ cm^{-2} are used without rechlorination of the surface, the Cl AES signal quickly decreases (Fig. 7). It falls below the AES sensitivity after 5 pulses, showing that the cumulated coverage in the first Si planes is below 10^{-2} ML, or that the concentration near the surface is lower than $\sim 5 \times 10^{20}$ cm^{-3}. Our TOF mass spectrometer is more sensitive than AES. The SiCl TOF peak decreases by more than 3 orders of magnitude in 8 laser pulses, and it is still measurable after a large number of pulses. Cleaning results from the desorption of a *fraction* of Cl at each pulse. In addition, this fraction becomes smaller as the number of laser pulses increases (Fig. 3). This may be due to the fact that Cl has not the time to diffuse in the entire melted surface layer during one laser pulse (the diffusion length being shorter than the melted depth at 600 mJ cm^{-2}): the undesorbed atoms are distributed in a broader layer after several laser pulses, thus increasing the fraction of undesorbed atoms. It might also be due to a lower segregation (or a segregation coefficient closer to unity) as the Cl density decreases, although the physical reason for that is not clear.

As mentioned in the experimental section, laser cleaning is efficient for C/Si also. We have observed that 100 laser pulses are sufficient to remove C (at the sensitivity of AES) from an air-exposed Si sample. Such an efficiency is not obtained for any element. For example, the O coverage decreases below the sensitivity level of AES after as much as 500 laser pulses. A C depth profile of a laser cleaned Si sample has been measured by SIMS in Ref. [38]. The Si sample contained initially a C coverage significantly lower than our initial Cl coverage of 1 ML during laser etching. The C depth profile after 20 laser pulses at 610 mJ cm^{-2} exhibits a surface peak of 5×10^{20} cm^{-3} (or 10^{-2} ML). The C concentration then reaches a plateau at 6×10^{19} cm^{-3} (~ 1 order of magnitude lower than the surface peak), and finally decreases after ~ 100 nm below the sensitivity level. A comparison of these numbers with our results for Cl show that Cl is even more efficiently removed than C: the surface peak height is $(3–7) \times 10^{20}$ cm^{-3}, the plateau, which is below the sensitivity level, is lower than the surface peak by at least 2 orders of magnitude for an initial coverage of 1 ML.

The efficiency of laser cleaning is related to the competition between diffusion to the bulk and desorption. This competition affects primarily the amount of impurities that remain in the substrate after the laser pulse. Segregation affects the location (surface peak versus plateau) of the remaining impurities in the melted layer. Because only those atoms that are located at the surface or very close to it can desorb at the next pulse, the strongest the segregation (the closest to zero the segregation coefficient), the largest the amount of impurity that can be desorbed at the next laser pulse. The comparison of C and Cl depth profiles shows that Cl has an even lower segregation coefficient than C: in the case of Cl, a fraction of $0.63 < D_{\text{AES}}/(D_{\text{AES}} + D_{\text{deep}}) < 1$ is in the surface layer, while for C, the amount is only ~ 0.10. The less favorable case of O from the point of view of laser cleaning can be related to the absence of segregation of O in Si during recrystallization [23].

4.6. Cl solubility in solid Si

The SIMS results show that the Cl solubility in solid Si is lower than 10^{19} cm^{-3}. A typical solubility for dopants in silicon is of the order of 10^{20} cm^{-3} for many elements [40]. Larger concentrations than the solubility may be achieved (for example, by ion implantation followed by laser annealing), but they may lead to severe defects. Arsenic has the largest

solubility of Si dopants (1.5×10^{21} cm^{-3}). Sb has a rather small solubility (7×10^{19} cm^{-3}). Since dopants have a more favorable electronic structure than Cl to insert into the Si crystal (number of electrons in the outer shell), and considering that the large size of Cl is also unfavorable for interstitial solubility, the low solubility of Cl in Si is not too surprising.

4.7. Desorption mechanism

The main results that are relevant to elucidate the desorption mechanism can be summarized as follows. The main desorption products are SiCl and $SiCl_2$ in the ratio of 1.3:1, while SiCl is not a desorption product in TPD experiments. The TOF spectra of SiCl and $SiCl_2$ are compatible with MB distributions at the Si melting temperature. Whether the surface is clean or has chlorine adsorbed on it from a previous pulse does not measurably influence the $SiCl/SiCl_2$ ratio or the etch rate. The desorption kinetics measured in TPD experiments and extrapolated to the conditions of laser desorption cannot account for the laser desorption yield which is 50 times larger than calculated [36]. In addition, laser desorption of dopant atoms during etching seems to be correlated with structural details of the solid surface [3].

There is no definite evidence that direct photo-induced processes are operative in laser desorption. The very short time scale (a few tens of nanoseconds) and the very high surface temperature ($\sim$ 2000 K) in laser induced desorption may open thermal desorption channels of large activation energy which are not operative in TPD. The TOF spectra of SiCl and $SiCl_2$ are compatible with MB distributions at the Si melting temperature of 1680 K and thus with a thermal desorption mechanism.

Desorption may occur at three stages of laser melting: before melting, during surface melting and during recrystallization:

(a) *Desorption before melting.* On the solid surface, $SiCl_2$ may desorb either by evaporation from dichlorinated sites (steps and other defects) or by surface reactions involving diffusion of Cl atoms towards reactive sites. The activation energy for such a surface reaction is expected to be lower than that of evaporation. In agreement with this, it is surface reactions that cause the desorption of $SiCl_2$ in TPD experiments. STM observations at 900 K show that these reactions occur mainly at steps [45]. However, as mentioned above, the reaction kinetics of these surface reactions [36] is too slow to account for the laser desorption yield of 0.15 to 0.20 ML. Therefore, $SiCl_2$ desorption is due to evaporation, or it occurs at the next stages of laser melting. $SiCl_2$ evaporation with a yield of roughly 0.2 ML would imply that the density of surface defects is $\sim$ 0.2 ML. This seems too large, because laser cleaned surfaces, which are obtained under the same conditions as laser etching, exhibit LEED patterns [38]. However, it might be that recrystallization in the presence of a significant density of Cl atoms produces a particular surface reconstruction with a large density of dichlorinated sites. If it would be the case, we would expect an increase of $\sim$ 0.2 ML of the saturation coverage after one laser pulse, rather than the observed 0.05 ML. We would also expect significant variations of the etch rate and of the SiCl to $SiCl_2$ ratio between the surface in permanent regime ($\mathcal{N} = 1$) and the almost clean surface ($\mathcal{N} = 8$), which is not supported by the TOF experiments. We conclude that $SiCl_2$ desorption occurs mainly during melting or during recrystallization.

SiCl is the main surface species. It may desorb by evaporation. Matsuo et al. have reported recently the onset of SiCl thermal desorption from Si(111) in isothermal desorption experiments at surface temperatures larger than 800°C [44], showing that SiCl desorption may be obtained without surface melting, at least on the (111) surface. It would seem reasonable to conclude that the opening of this thermal desorption channel in the temperature range 800°C–1400°C is responsible for SiCl desorption in our laser experiments. Unfortunately, the desorption kinetics of SiCl was not measured by Matsuo et al.

There is another argument in favor of desorption before melting: desorption before melting is the only case where structural details of the initial surface may play a role. The relative desorption efficiencies of Sb, As, and B dopants seem to be correlated with the existence of islands and of surface dimers [3]. Thus, at least dopant desorption seems to be faster than the complete melting of these structures into the Si liquid layer.

However, the desorption yield decreases so

sharply as the laser fluence decreases below the melting threshold [11] that it is dubious that any significant desorption is obtained without melting. These two conclusions can only be reconciled if we admit that a significant increase of the desorption yields is produced at the early stages of laser melting, before the adsorbates lose memory of the surface structure.

(b) *Desorption during surface melting.* Melting has the effect to induce very efficiently diffusion towards the bulk. It is surface melting that prevents desorption of a significant fraction of chlorine atoms during the laser pulse. Consequently, we expect a large decrease of adsorbate coverages during melting, with the effect of a significant reduction of evaporation at this stage.

(c) *Desorption after surface melting.* Given the large number of Cl atoms (the equivalent of at least 0.3 ML) that come to the surface from the bulk at the end of recrystallization, while the surface is still very hot (1680 K), desorption of Si chlorides at this stage seems likely. There is no reason at this stage that desorption of monochlorides would be favored over desorption of dichlorides. Diffusion (which limits the reactivity on the solid surface) is expected to be orders of magnitude larger on the liquid than on the solid, while evaporation of $SiCl_2$ is energetically favored over evaporation of SiCl. Therefore, a burst of $SiCl_2$ molecules after the laser pulse seems quite realistic.

5. Summary and conclusion

This work bears out direct evidence of Cl diffusion to the bulk in the course of laser etching experiments of Si by Cl, under conditions of surface melting. By measuring the Si and SiCl desorption yields, the remaining Cl dose near the surface, and by setting an upper limit on the amount of Cl deeper in the bulk, we are able to estimate the branching ratios for reactive (SiCl, $SiCl_2$) and unreactive (Cl, Cl_2) desorption, and for diffusion near the surface or deeper (Table 2). Reactive desorption is dominant with respect to unreactive desorption, and the ratio between the two desorption products $SiCl/SiCl_2$ is ~ 1.3. About 60% of adsorbed Cl desorb reactively, while about 30% diffuse to the bulk. Although laser melting induces diffusion to the bulk, strong segregation of Cl at the liquid/solid Si interface during recrystallization limits Si contamination to low levels ($< 10^{19}$ cm^{-3}). A majority of those Cl atoms which have diffused to the bulk are found *at* the surface after recrystallization. Cl on Si is in fact a very favorable case for laser cleaning.

There is no experimental evidence that photo-induced processes play a direct role in laser etching under the conditions of surface melting. Instead, etching seems to result from competing, "fast" thermal processes (with respect to the thermal desorption that occurs in TPD experiments): at the beginning of the laser pulse, at the very early stages of surface melting, evaporation of SiCl is likely to occur from terraces while $SiCl_2$ desorption would be limited to evaporation at defect sites. Surface reactions are too slow to account for the $SiCl_2$ desorption yield. During surface melting, diffusion to the bulk competes efficiently with desorption with the result of "pumping" Cl atoms towards the bulk. After the laser pulse, the surface recrystallizes. At this stage, segregation brings most of Cl atoms back to the surface. A fraction of them might desorb in the form of $SiCl_2$.

The consequences of these results for applications in microelectronics are of two kinds. They explain why the etch rate is limited to 0.4 Si ML/pulse under the conditions of surface melting, while at saturation, the Si:Cl ratio is one on Si(100). One might expect a maximum etch rate of 1 Si ML/pulse, which is not observed. The limited saturation etch rate results mainly from the competition between desorption and diffusion to the bulk: those Cl atoms that diffuse to the bulk are no longer available for reactive desorption. Unreactive desorption also contributes (but to a lesser extent) to the limitation of the etch rate. The etch rate remains significant anyway, similar to the rate that may be obtained at laser fluences below the melting threshold by reactive scattering of gas phase chlorine at the surface. The laser melting/etching mechanism has the advantage to require significantly lower Cl pressures. 10^{-3} mbar (and much less with a molecular beam) is enough to saturate the surface between two laser pulses, while 100 mbar is necessary to reach a collision rate of 1 per Si atom during a laser pulse of 20 ns.

The other implication of the present results is that

laser cleaning is very efficient for Cl on silicon. Although laser melting does induce diffusion of Cl to the bulk, it does not cause significant bulk contamination because of segregation. The (weakly) contaminated depth can be limited by adjusting the laser fluence so as to minimize the melted depth. In addition, the laser can be used at the end of the surface processing to clean the bulk.

Acknowledgements

M.S. is very much indebted to the Ministère de la Recherche et de la Technologie (France) for a post-doctoral grant. The SIMS measurements were made using the facilities of the CEETAM (Centre d'Etudes et d'Education des Techniques Avancées de la Micro-électronique) by J.-B. Ozenne.

References

[1] D. Bäuerle, Chemical Processing with Lasers, Vol. 1 of Springer Series in Materials Science (Springer, Berlin, 1986).
[2] I.W. Boyd, Laser Processing of Thin Films and Microstructures, Springer Series in Materials Science 3 (Springer, Berlin, 1987).
[3] A. Desmur, B. Bourguignon, J. Boulmer, J.-B. Ozenne, J.-P. Budin, D. Débarre and A. Aliouchouche, J. Appl. Phys. 76 (1994) 3081;
J. Boulmer, A. Desmur, B. Bourguignon, J.-B. Ozenne, R. Laval, A. Aliouchouche, D. Débarre and J.-P. Budin, Mater. Sci. Forum 173 174 (1995) 23.
[4] R. Tsu, D. Lubben, T.R. Bramblett and J.E. Greene, J. Vac. Sci. Technol. A 9 (1991) 223.
[5] J. Boulmer, B. Bourguignon, J.-P. Budin and D. Débarre, Appl. Surf. Sci. 43 (1989) 424.
[6] J. Boulmer, B. Bourguignon, J.-P. Budin and D. Débarre, Chemtronics 4 (1989) 165.
[7] B. Bourguignon, J. Boulmer, J.-P. Budin and D. Débarre, in: DIET IV, Vol. 19 of Springer Ser. Surf. Sci., Eds. G. Betz and P. Varga (1990) p. 147.
[8] J. Boulmer, B. Bourguignon, J.-P. Budin and D. Débarre, Ann. Phys. 15 Coll. N° 3, Suppl. N° 3 (1990) 3.
[9] J. Boulmer, B. Bourguignon, J.-P. Budin, D. Débarre and A. Desmur, J. Vac. Sci. Technol. A 9 (1991) 2923.
[10] J. Boulmer, J.-P. Budin, B. Bourguignon, D. Débarre and A. Desmur, in: Laser Ablation of Electronic Materials, Eds. E. Fogarassy and S. Lazare (Elsevier, Amsterdam, 1992) p. 239.
[11] A. Aliouchouche, J. Boulmer, B. Bourguignon, J.-P. Budin, D. Débarre and A. Desmur, Appl. Surf. Sci. 69 (1993) 52.
[12] R. Kullmer and D. Bäuerle, Appl. Phys. A 43 (1987) 227.
[13] P. Mogyorosi, K. Piglmayer, R. Kullmer and D. Bäuerle, Appl. Phys. A 45 (1988) 293.
[14] R. Kullmer and D. Bäuerle, Appl. Phys. A 47 (1988) 377.
[15] T.S. Baller, J.C.S. Kools and J. Dieleman, Appl. Surf. Sci. 46 (1990) 292.
[16] H. Feil, T.S. Baller and J. Dieleman, Appl. Phys. A 55 (1992) 554.
[17] W. Sesselmann, E. Hudeczek and F. Bachmann, J. Vac. Sci. Technol. B 7 (1989) 1284.
[18] Y.-L. Li, Z.-J. Zhang, Q.-K. Zheng, Z.-K. Jin, Z.-K. Wu and Q.-Z. Qin, Appl. Phys. Lett. 53 (1988) 1955.
[19] Y.-L. Li, Q.-K. Zheng, Z.-K. Jin, M. Yu, Z.-K. Wu and Q.-Z. Qin, J. Phys. Chem. 93 (1989) 5531.
[20] Q.-Z. Qin, Y.-L. Li, P.H. Lu, Z.-J. Zhang, Z.-K. Jin and Q.K. Zheng, J. Vac. Sci. Technol. B 10 (1992) 201.
[21] F.X. Campos, G.C. Weaver, C.J. Waltman and S.R. Leone, J. Vac. Sci. Technol. B 10 (1992) 2217.
[22] C.N. Rhodin, C. Paulsen-Boaz and W.L. O'Brien, Surf. Sci. 283 (1993) 109.
[23] B. Leroy, Rev. Phys. Appl. 21 (1986) 467.
[24] C.W. White, P.P. Pronko, S.R. Wilson, B.R. Appleton, J. Narayan and R.J. Young, J. Appl. Phys. 50 (1979) 3261.
[25] C.W. White, S.R. Wilson, B.R. Appleton and F.W. Young, Jr., J. Appl. Phys. 51 (1980) 738.
[26] R.F. Wood and G.E. Giles, Phys. Rev. B 23 (1981) 2923.
[27] R.F. Wood, J.R. Kirkpatrick and G.E. Giles, Phys. Rev. B 23 (1981) 2923.
[28] R.F. Wood, Phys. Rev. B 25 (1982) 2786.
[29] S.U. Campisano, Appl. Phys. A 30 (1983) 195.
[30] E. Fogarassy, in: Energetic Beam Solid Interactions and Transient Thermal Processing, Eds. V.J. Nguyen and A.G. Cullis (Éditions du Physique, Paris, 1985) p. 153.
[31] A. Szabo, P.D. Farrall and T. Engel, Surf. Sci. 312 (1994) 284.
[32] R.B. Jackman, H. Ebert and J.S. Foord, Surf. Sci. 176 (1986) 183.
[33] J.E. Rowe, Surf. Sci. 53 (1975) 461.
[34] M. Schlüter, J.E. Rowe and G. Margaritondo, Phys. Rev. Lett. 37 (1976) 1632.
[35] J.E. Rowe, G. Margaritondo and S.B. Christman, Phys. Rev. B 16 (1977) 1581.
[36] J.V. Florio and W.D. Robertson, Surf. Sci. 18 (1969) 398.
[37] N. Aoto, E. Ikawa and Y. Kurogi, Surf. Sci. 199 (1988) 408; L.S.O. Johansson, R.I.G. Uhrberg, R. Lindsay, P.L. Wincott and G. Thornton, Phys. Rev. B 42 (1990) 9534.
[38] R. Tsu, D. Lubben, T.R. Bramblett and J.E. Greene, J. Vac. Sci. Technol. A 9 (1991) 223.
[39] R. Kelly and R.W. Dreyfus, Surf. Sci. 198 (1988) 263.
[40] C.W. White, J. Phys., Coll. C 5, Suppl. 10, 44 (1983) 145.
[41] F. Foulon, in: Photochemical Processing of Electronic Materials, Eds. I.W. Boyd and R.B. Jackman (Academic Press, London, 1992) p. 257.
[42] M.P. Seah, in: Practical Surface Analysis, Eds. D. Briggs and M.P. Seah (Wiley, Chichester, 1983) p. 186.
[43] R.G. Wilson, F.A. Steve and C.W. Magee, Secondary Ion Mass Spectrometry. A Practical Handbook for Depth Profiling and Bulk Impurity Analysis (Wiley, New York, 1989) Appendix E, p. 22.
[44] J. Matsuo, Y. Feurprier and K. Karahashi, Surf. Sci. 283 (1993) 52.
[45] A. Feltz, U. Memmert and R.J. Behm, Surf. Sci. 307–309 (1994) 216.